Visible Wavelength PICs for Fluorescent Microscopy and Flow Cytometry

Alireza Tabatabaei Mashayekh,[1] Florian Merget,[1] Martin Büscher,[2] Thomas Klos,[3] Marc Spehr,[4] Douwe Geuzebroek,[5] Jeremy Witzens[1,*]

[1]*Institute of Integrated Photonics, RWTH Aachen University, Campus Blvd. 73, 52074 Aachen, Germany*
[2]*Miltenyi Biotec, Friedrich-Ebert-Straße 68, 51429 Bergisch Gladbach, Germany*
[3]*Toptica Photonics AG, Lochhamer Schlag 19, 82166 Gräfelfing, Germany*
[4]*Chemosensation Laboratory, RWTH Aachen University, Worringerweg 3, 52074 Aachen, Germany*
[5]*LioniX International BV, Hengelostraat 500, 7521 Enschede, The Netherlands*
jwitzens@iph.rwth-aachen.de

Abstract: We present two multi-color laser engines for fluorescent confocal microscopy and polychromatic flow cytometry implemented in silicon nitride PICs. Besides miniaturization, PICs facilitate structured illumination, used here to distinguish fluorescent signals by excitation wavelength. © 2022 The Author(s)

1. Introduction

Visible wavelength photonic integrated circuits (PIC) enable the miniaturization of conventional multi-color laser engines (MLE) [1], a core element of biomedical imaging and diagnostic tools. This results in robust and compact solutions with fewer discrete components. In addition, PICs can facilitate volumetric 3D imaging techniques with sub-cellular resolution, such as light sheet fluorescent microscopy (LSFM). Higher data acquisition speeds and lower phototoxicity are afforded by a mm-scale field of view combined with sub-cellular resolution and the complexity of bulky and expensive discrete assemblies can be reduced [2]. We present two miniaturized PIC-based MLEs using the TripleX silicon nitride (SiN) single-stripe platform with an optimized SiN layer thickness of ~26 nm [3]. The first MLE provides the same functionality as commercial devices operating at the commonly used 405, 488, 561, and 640 nm excitation wavelengths in a much smaller form factor [4]. The second generates structured illumination patterns for polychromatic flow cytometry (PFC) [5]. Spatially overlapping excitation patterns focused on the sample flow result in a unique time domain signature that serves to attribute the fluorescence and scattering signals to their excitation wavelengths.

2. SiN PIC-based multi-color laser engines for fluorescent imaging and flow cytometry

The architecture of the first PIC-based MLE is shown in Fig. 1(a). It implements wavelength multiplexing, power tuneability, and switching over a pair of fiber outputs to switch between illumination modalities. To couple light into the PIC, a pair of convex lenses are interposed between the chip and the laser sources, for collimating and then focusing the light at the input facet. All these are assembled on a mechanical stage. The low-confinement on-chip waveguides are optimized for transverse magnetic (TM) light and allow a low insertion loss (IL) at chip-to-fiber interfaces at the output ports of the PIC. Laser diodes (LDs) directly generate the three wavelengths 405, 488, and 640 nm. Since LDs are not readily available at 561 nm, a frequency-doubled diode laser (FDDL) sources this wavelength. For each of the wavelengths, thermally tuned Mach-Zehnder interferometers (MZIs) with differential output implement both variable optical attenuation and splitting of the light over the two output fibers. Each MZI-based switch consists of a 1-by-2 and a 2-by-2 multi-mode interferometer (MMI) and two thermal phase tuners with kHz modulation speed embedded in the interferometer branches. Wavelength combiners (WLCs) consist in cascaded symmetric directional couplers (DC) and multiplex the MZI outputs [Fig. 2(a)]. Finally, the light is out-coupled to a fiber array (FA) attached to the output edge couplers [inset in Fig. 1(a)]. The layout of the PIC-based MLE is shown in Fig. 1(b). The PIC has an extinction ratio above 10 dB for all wavelengths, ILs of 6 ± 1 dB at 488, 561, 640 nm, and 12 ± 1 dB at 405 nm, and requires actuation voltages below 15 V. ILs at 405 nm in particular can be improved by retargeting the edge couplers. A simpler version of the miniaturized PIC-based MLE has also been demonstrated with a single fiber output [6].

The architecture of the second PIC-based MLE is shown in Fig. 1(c). It generates illumination patterns with wavelength dependent periodicities and is aimed at polychromatic flow cytometry. The PIC layout is shown in Fig. 1(d), including 1-by-2 MMIs splitting the light for each wavelength, as two output ECs are required for each to generate the interferometric pattern. As above, symmetric DC-based WLCs combine 405 nm with 488 nm and 561 nm with 640 nm to reduce the number of output ports. The output ECs, as shown in the inset of Fig. 1(d), are tapered to a 3.6 μm width to obtain the targeted beam diffraction and are spaced (edge to edge) by 36.58 μm (405/488 nm) and 74 μm (561/640 nm) to obtain the targeted illumination periodicities. External beam-shaping optics consist in a

set of three lenses. The first two magnify the output of the waveguides onto an image plane 61.7 mm from the PIC edge, increasing the distance between the correspond spots by 136x. A cylindrical lens placed close to the flow channel then deflects the beams to create the interferometric pattern along the axis of the flow channel. Its full-width at half maximum is targeted to be 300 µm along the flow channel and 60 µm along the other directions, the latter accommodating some variability of the cell positions inside the flow. An IL of 7.5, 5.25, 3.25, and 3.9 dB is determined at 405, 488, 561, and 640 nm, respectively. Similar laser sources and interposed in-coupling lenses are used as in the previous MLE, with a slight modification of the mechanical stage allowing for the assembly of the beam shaping optics [inset in Fig. 1(a)]. This PIC is also designed to operate with TM-polarized light.

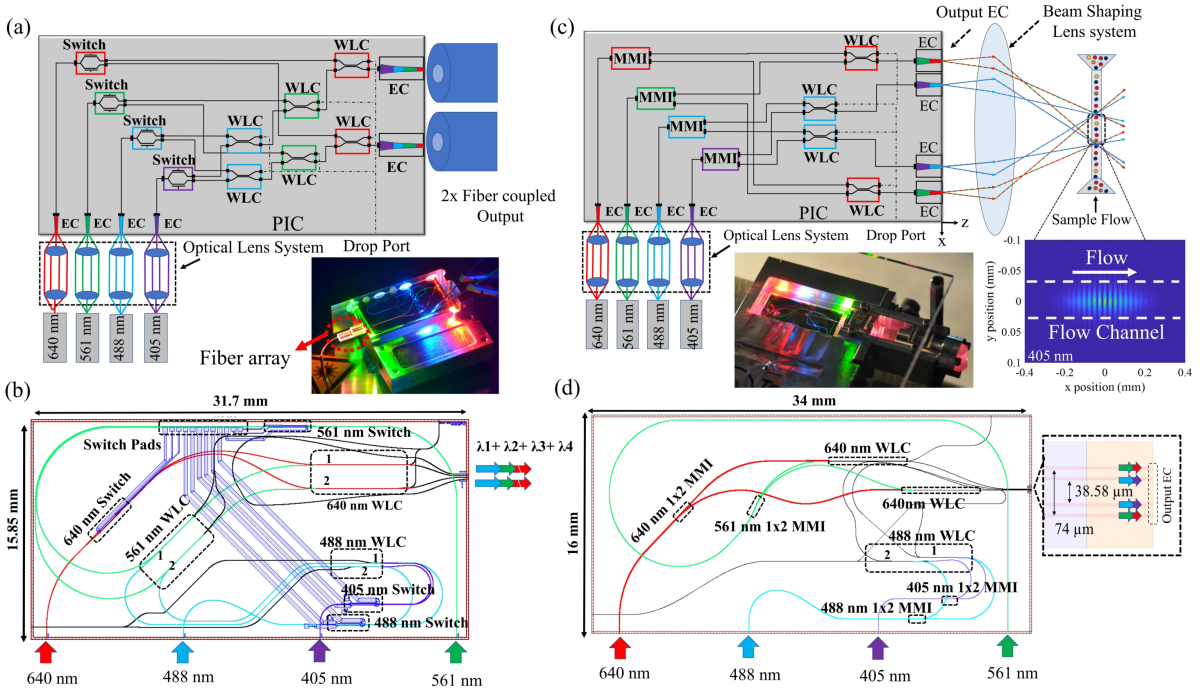

Fig. 1. (a) Architecture and (b) PIC-layout of the dual fiber output MLE. The inset in Fig. 1(a) shows a photograph of the assembled MLE with attached FA. (c) Architecture and (d) PIC-layout of the structured illumination MLE for PFC. The left inset in (c) shows a photograph of the assembled MLE with auxiliary beam forming optics. The right inset shows the simulated interferometric pattern at the position of the flow channel at 405 nm. Adapted with permission from [4] and [5].

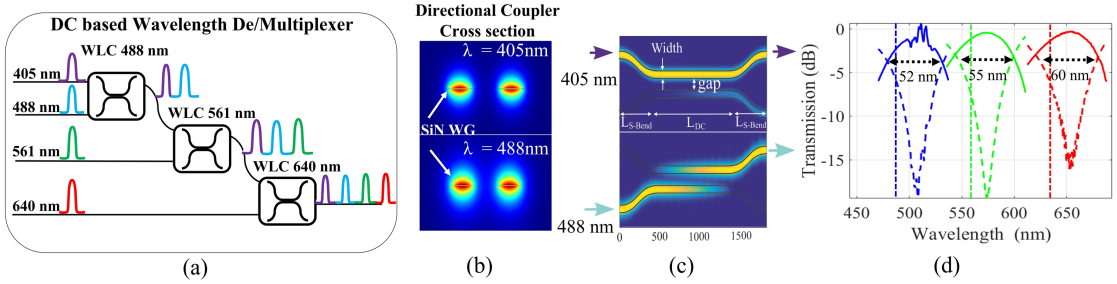

Fig. 2. (a) Schematic of the cascaded combiner stages used in the first PIC, (b) simulated lowest order super-mode intensity profile in WLC488 at 405 and 488 nm, showing the high confinement at the shorter wavelength, (c) simulation of the light propagation through WLC488 at 405 and 488 nm (color maps indicate the field intensity). (d) Measurement results. Adapted with permission from [4].

An excess loss below 1.5 dB is measured from test structures for the 1x2 and 2x2 MMIs used to implement both PICs. The symmetric 1x2 MMIs feature negligible output power imbalance; however, the 2x2 MMIs currently suffer from a higher imbalance (~20 %), that could be improved by retargeting of the device length. In the first MLE, a cascade of DC-based WLCs multiplexes the four wavelengths, see Fig. 2(a), adding sequentially 488 to 405 nm, 561 to the other two, and 640 nm to the previous three. The naming of the devices is based on the next longer wavelength added by the combiner to the bus waveguide. The waveguides inside the directional couplers are sized to provide high confinement and thus low evanescent coupling for the shorter wavelengths, and low confinement for the longer wavelength added to the bus, such that near 100% coupling of the longer wavelength can be achieved

without perturbing the propagation of the shorter wavelengths remaining in the bus. This way, a multiplexer operation over a 235 nm range is achieved. Fig. 2(d) shows the spectral responses of test devices featuring 3-dB bandwidths of ~52, ~55, and ~60 nm for the add-ports of WLC488, WLC561, and WLC640, respectively. Due to process bias, the passbands are shifted by ~20 nm from target, leading to ILs below 2 dB at the laser wavelengths.

3. Characterization of PFC using PIC-based MLE with structured illumination

The schematic of the fully assembled PFC using PIC-based structured illumination is shown in Fig. 3(a). It consists of the optical subassembly, combined with electronics for driving the laser diodes, flanged onto the flow cell comprising a quartz cuvette in which the interferometric pattern interacts with hydrodynamically focused particles. An adjustable objective lens oriented orthogonally to the laser beams collects the fluorescent and side scattering (SSC) signals of the passing particles. The collected beam size is reduced with a pair of lenses and split with a 90:10 beam splitter between a photomultiplier tube (PMT) recording the SSC signal (10%) and a multi-band filter eliminating the pump beams prior to the fluorescent signals being recorded by a second PMT (90%). To assess common fluorescence channels at different staining levels, a mixture of stained and unstained particles with a diameter of 3.8 ± 0.2 (SPHERO™ Ultra Rainbow Calibration Particle Kit, Cat. No. URCP-38-2K) is utilized with a concentration of 500 particles per µL. The stained particles contain the four fluorophores Coumarin 30, fluorescein isothiocyanate (FITC), Nile Red, and allophycocyanin (APC), with main absorption peaks at 405, 488, 550, and 651 nm close to the wavelengths of the utilized laser sources, at five intensity levels.

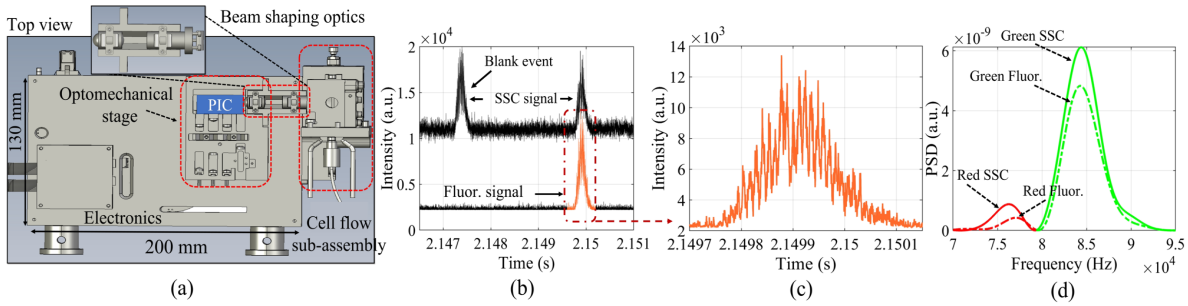

Fig. 3. (a) Diagram of PIC-based PFC, (b) exemplary recorded time-domain PMT signals, including the SSC (upper curve) and fluorescent (lower curve) signals. The first event corresponds to an unstained particle, the second to a stained one. (c) Fluorescent signal resulting from the stained particle, (d) PSD of the SSC and fluorescent signals with the 561 and 640 nm lasers turned on. Source: Adapted with permission from [5].

Exemplary SSC and fluorescence signals recorded with the 561 and 640 nm lasers turned on are shown in Fig. 3(b). They consist of two events, the recording of an unstained and a stained particle with fluorescence signal. The details of the fluorescence signal containing the response to both excitation wavelengths is shown in Fig. 3(c). The power spectral densities (PSD) of the selected SSC and fluorescent signals are shown in Fig. 3(d) and contain two distributions centered on 85.3 and 76 kHz. Since the particles travel with a fixed speed through the flow channel, the spatial periodicity of the excitation beams is converted into a well-defined temporal periodicity in the recorded responses, so that their spectral components can be unambiguously attributed to the excitation wavelengths.

As an outlook, we are currently investigating the generation of structured illumination patterns with PIC-based optical phased arrays (OPA) for LSFM [2].

4. Conclusion

We presented two types of miniaturized SiN PIC-based MLEs operating at 405, 488, 561, and 640 nm offering more robust and compact solutions for confocal fluorescent microscopy and flow cytometry, with a reduced number of discrete components afforded by on-chip integration. This may also lower the expense of equipment to a level compatible with point-of-care clinical trials.

References

[1] S. Romero-García *et al.*, "Photonic integrated circuits for multi-color laser engines," Proc. SPIE **10108**, 10108Z (2017).
[2] J. Witzens, M. Spehr, P. Van Dorpe, and N. Verellen, "Enhanced field-of-view high-resolution lattice light sheer microscopy with phased array beam formers," Proc. SPIE **11652**, 1165207 (2021).
[3] K. Wörhoff, R. G. Heideman, A. Leinse, and M. Hoekman, "TriPleX: a versatile dielectric photonic platform," Adv. Opt. Technol. **4**(2), 189-207 (2015).
[4] A. Tabatabaei Mashayekh *et al.*, "Silicon nitride PIC-based multi-color laser engines for life science applications," Opt. Express **29**(6), 8635-8653 (2021).
[5] A. Tabatabaei Mashayekh *et al.*, "Multi-color flow cytometer with PIC-based structured illumination," Biomed. Opt. Express **13**(10), 5098-5115 (2022).
[6] A. Tabatabaei Mashayekh *et al.*, "Miniaturized PIC multi-color laser engines for the life sciences," Proc. SPIE **10922**, 109221U (2019).